Infrared spectra of synthetic almandine–grossular and almandine–pyrope garnet solid solutions: evidence for equivalent site behaviour

C. A. GEIGER, B. WINKLER AND K. LANGER

Institut für Mineralogie und Kristallographie, Technische Universität Berlin, Ernst Reuter-Platz 1, D-1000 Berlin 12, Germany

Abstract

The infrared (IR) spectra of almandine–grossular and almandine–pyrope garnet solid solutions have been measured using the powder method. Frequency shifts of a band related to internal vibrations associated with the 8-co-ordinate dodecahedral site are nonlinear in almandine–grossular garnets and mimic the form of its molar volume of mixing curve. Almandine–pyrope solid solutions have nearly ideal molar volumes of mixing and the frequency shift of this same 8-co-ordinate site-related band is linear. The IR data support the empirically based crystal chemical model of Equivalent Site (ES) behaviour (Newton and Wood, 1980). The IR spectra give no indication of long-range ordering between Ca and Fe^{2+} in garnet, but thermodynamic calculations involving Ca-poor garnets might be affected by small volume or short-range ordering anomalies.

KEYWORDS: equivalent site behaviour, synthetic garnets, infrared spectroscopy, molar volumes of mixing.

Introduction

THE link between the thermodynamic properties and the microstructural constitution of complex phases is an active area of research in solid-state physics, the material sciences, and mineralogy. The macroscopic thermodynamic properties of a phase are governed by composition, structure, and atomic vibrations. Molar enthalpies of formation, molar volumes, or, to a greater degree, the mixing properties of silicate solid solutions, cannot be precisely calculated *a priori*, presently, but must be measured experimentally. There are, however, empirically based rules or guidelines that can often be applied to constrain or estimate thermodynamic properties. For example, a crystal chemically based model has been successful in explaining the systematics of the free energies of mixing of various spinel solid solutions (O'Neill and Navrotsky, 1984).

Newton and Wood (1980) developed a crystal chemical model to explain the detailed molar volume of mixing (ΔV^{mix}) behaviour of many silicate and oxide solid solutions, following upon the work of Iiyama (1974) and Iiyama and Volfinger (1976). The Newton and Wood model proposes that asymmetry in the ΔV^{mix} results, when solid solution occurs in a single site or nearly identical crystallographic sites, between two end-member components which have substantial differences in their molar volumes. The asymmetry is such that negative or nearly ideal behaviour is observed towards the small-volume end-member component, which changes to positive deviations from ideality farther away from the small-volume component. This behaviour in the molar volumes of mixing has been demonstrated in almandine–grossular (Cressey *et al.*, 1978) and in pyrope–grossular (Haselton and Newton, 1980) garnet solid solutions, where mixing occurs in the single 8-co-ordinate *X*-site. It is not present or is not so strongly developed along the almandine–pyrope join, because almandine and pyrope have relatively similar molar volumes (Geiger, 1986).

We have measured the infrared (IR) spectra of almandine–grossular (Al–Gr) and almandine–pyrope (Al–Py) garnets to investigate the internal site motions in these two solid solution series. There have been several previous IR studies on natural (Moore *et al.*, 1971, and Tarte, 1965) and synthetic (Delany, 1981) garnets which permit definitive assignment of most of the bands to the three different polyhedral sites in the garnet

Mineralogical Magazine, April 1989, Vol. 53, pp. 231–7

TABLE 1. Band positions in cm^{-1} for infrared spectra of $Al_{100-x}Gr_x$ and $Al_{100-y}Py_y$ garnets. Compositions are in mol%. The positions in the top row for each band were measured on the grating spectrometer, those in the bottom row were measured on the FTIR spectrometer. Blanks correspond to bands not observed.

Band \ x	0	05	10	15	40	50	65	75	90	100
B	965	963	961	958	949	943	938	929	920	913
	963	961	959	957	948	942	935	929	919	911
C	901	899	898	894	884	881	875	870	865	860
	900	899	896	894	884	880	874	870	864	860
D	878	877	874	873	868	862	858	852	846	843
	877	876	875	873	866	863	857	852	847	843
E	635	635	634	634	629	627	625	624	621	620
				633	629	628	625	624	621	
F	567	566	565	564	559	557	553	550	546	544
	566	565	564	562	558	556	553	550	546	543
G	527	524	521	521		512	510	512	512	509
	526	526							515	506
H	471	472	472	473	476	475	476	476	474	475
	470	472	472	473	475	475	474	475	474	473
I	450	451	451	451	454	452	453	452	452	451
	450	451	451	450	454	452	453	452	450	451
J										
K	376	378	378	380	390	392	396	397	396	396
	375	375	379	380	392	394	395	397	395	396
L	340	342	345	342						355
	340		343							
M	315	316	315	316					298	300
	315		314	316						302

Band \ y	0	07	15	25	40	50	62	75	90	100
B	965	965	967	968	970	972	973	973	975	976
	963	964	965	967	969	970	971	973	975	976
C	901	902	902	903	904	905	905	906	907	907
	900	901	901	902	903	903	904	905	906	906
D	878	878	878	878	878	878	878	878	878	877
	877	876	877	877	877	877	877	877	876	876
E	635	637	638	639	643	642				
		635	637		641					
F	567	568	569	571	574	575	578	581	582	585
	566	567	569	570	573	575	577	580	581	583
G	527	528	528	529	532	533	535	537	538	539
	526	527	528	529	531	532		536	538	538
H	471	472	473	475	477	478	480	480	482	482
	470	472	472	475	476	477	478	479	481	482
I	450	451	453	454	455	458	459	460	463	463
	450	451	452	454	456	458	459	461	463	462
J					413	416	415	419	420	420
					417			418	421	
K	376	377	378	379	381	383	383	384	386	386
	375	377	378	379		382	383	384	386	386
L	340	340	341	341	342	342	336	337	340	339
	340	340	341	343		343	335	336	340	339
M	315	318	321	325	329					
	315	318	324	324		328				

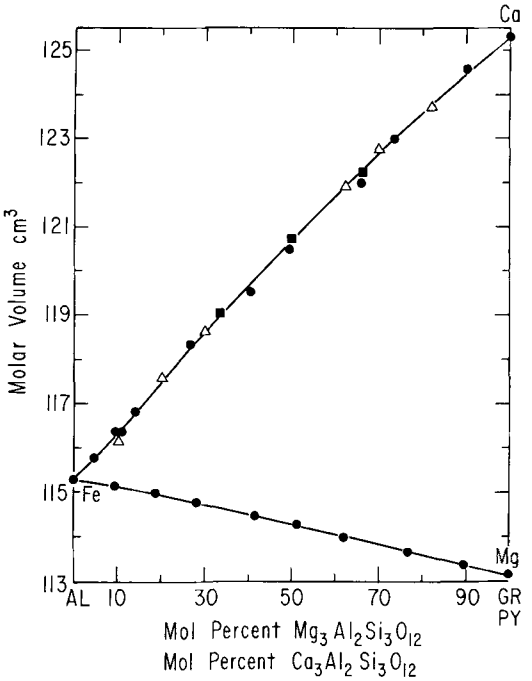

FIG. 1. Unit-cell volumes of binary almandine (Al)–grossular (Gr) and almandine–pyrope (Py) solid solutions. The symbol sizes are larger than the errors. Solid circles: Geiger *et al.*, 1987; solid squares: Perkins, 1979; open triangles: Cressey *et al.*, 1978. Al–Gr solid solutions display ES behaviour, while Al–Py have molar volumes which are nearly ideal.

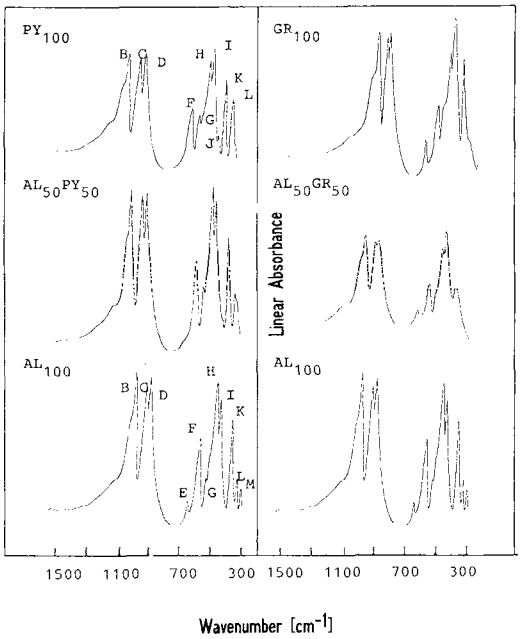

FIG. 2. Representative IR spectra of almandine (Al)–grossular (Gr) and almandine–pyrope (Py) garnets, plotted as linear absorbance *vs.* wavenumber in cm^{-1} from 1500 cm^{-1}–300 cm^{-1}. The compositions are given in the upper left hand corner. Bands are labelled for end-member Py and Al.

structure. However, a detailed study covering the entire binary join of well characterized synthetic solid solutions has not been undertaken. Therefore, we have examined the various IR bands for possible splittings and have analysed their positions and shifts as a function of composition across both joins. We also examined and plotted the band shifts to see if they are consistent with, or might help interpret, the molar volumes of mixing behaviour of these two garnet joins.

Experimental procedure

Synthetic, polycrystalline Al–Gr and Al–Py solid solutions were synthesized from mechanical mixtures of the end-member glasses at 1423 K and 27 kbar and 1523 K and 28 kbar, respectively, in a piston-cylinder device (Geiger *et al.*, 1987). The syntheses were done anhydrously in graphite capsules to ensure a low fO_2 and to avoid any incorporation of OH^- into the garnets (Geiger, unpublished data). The garnets were characterized by optical microscope, electron microprobe, Mössbauer and X-ray diffraction studies, which determined their compositions and stoichiometries. Samples were X-rayed with an internal spinel standard to calculate the unit-cell dimension a_0 (Geiger *et al.*, 1987). For IR spectroscopic investigations, pressed disks of 13 mm diameter were prepared, using 2 mg of preground garnet and 300 mg of CsI. Duplicate spectra were measured on a Perkin-Elmer 580B grating spectrometer and on a Fourier transform MX-1 Nicolet spectrometer. The operating conditions for the Perkin-Elmer Spectrometer were the following, maximum resolution 2.3 cm^{-1}, relative noise 0.3, and a scan time from 1500–200 cm^{-1} of 10 minutes, and for the Nicolet, resolution 2 cm^{-1} and 32 averaged scans.

Results

The unit-cell data were used, with existing data on Al–Gr solid solutions (Perkins, 1979, and Cressey *et al.*, 1978), and with the data on Al–Py garnets to construct the molar volume curves shown in Fig. 1. The molar volumes show a little scatter, but the general trend of all the data is clear. The smoothed curves represent a subregular fit to the data (Newton *et al.*, in press).

The bands in the IR region that we observed, in these synthetic materials, have been also found in IR studies made on natural garnets (Moore *et al.*, 1971 and Tarte, 1965). All band shifts

changed in a systematic way and no splittings were observed. Several representative IR spectra for both binaries in the region of 1500–300 cm^{-1} are shown in Fig. 2. Slight band broadening in certain samples may be related to small compositional inhomogenities (e.g. $Al_{50}Gr_{50}$—see Fig. 2). The agreement in band positioning between the two spectrometers was good and did not differ by more than 2 cm^{-1} for a given band, with the exception of three cases. Table 1 lists the band positions.

Discussion

The general aluminosilicate garnet formula is $X_3Al_2Si_3O_{12}$, where X = Fe^{2+}, Mg, or Ca. For compositions investigated here, changes in the spectra should only be related to compositional differences in the X-site polyhedra (Fig. 3). Theoretical factor group analysis on garnet of space group *Ia3d* indicates that there is a total of 17 infrared active bands (Moore *et al.*, 1971), and we observed 12 (Al–Gr) and 13 (Al–Py) bands in the range of 1000–300 cm^{-1}. This is in agreement with previous IR studies and we use a similar band labelling scheme (Delany, 1981; Moore *et al.*, 1971; Tarte, 1965). There is some disagreement regarding the labelling of bands below 400 cm^{-1}, but this does not affect our results. The band labels (B–K) are shown in Fig. 2. The bands assigned to internal vibration of the three polyhedra of the garnet structure are, except for the two bands E and J, unambiguous. Bands B, C and D belong to ν_3 of the $[SiO_4]$ groups, bands F and G to $\nu_2 + \nu_4$ of the $[SiO_4]$ groups, where ν_3 is the asymmetric Si–O stretch and ν_2 and ν_4 are symmetric and asymmetric bending modes (Tarte, 1965, and Moore *et al.*, 1971). Band K may be assigned to vibrations in the dodecahedral $[XO_8]$ site and bands H and I to octahedral $[AlO_6]$ groups (Moore *et al.*, 1971). The positions of bands B–M for both solid solutions are plotted in cm^{-1} *vs.* composition in Fig. 4. Bands B, C and D show a strong shift of decreasing frequency of 35–50 cm^{-1}, with increasing mole percent of Gr (mol.% Gr), that is $\Delta\nu/\Delta x \simeq -0.35$ to -0.50 cm^{-1}/mol.% and a small increase of 0–11 cm^{-1} with increasing mol.% Py $\Delta\nu/\Delta x \approx 0.00$ to -0.11 cm^{-1}/mol.%. Band K increases with a maximum shift of 20 cm^{-1} in Al–Gr garnets and 10 cm^{-1} in Al–Py garnets. The magnitude of the shift of band K, compared to those of the internal $[SiO_4]$ vibrations, suggests that the tetrahedral groups are coupled relatively strongly to the rest of the structure (Fig. 3). Each tetrahedron shares two edges with two dodecahedra and, therefore, the substitution of different sized cations in the X-site affects the internal vibration characteristics

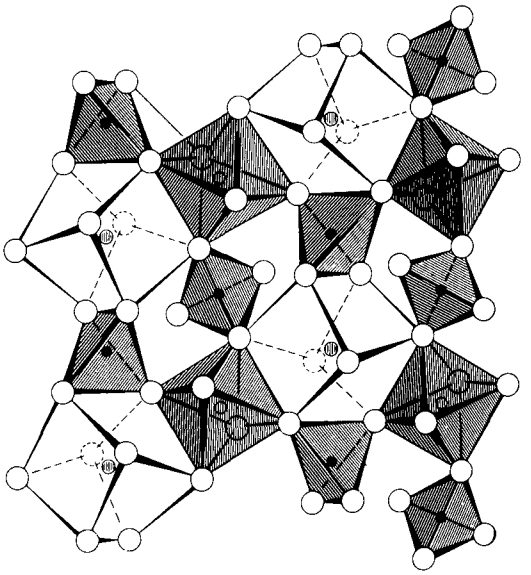

FIG. 3. Polyhedral model of the garnet structure (Novak and Gibbs, 1971). The octahedra and tetrahedra are lined.

of the $[SiO_4]$ tetrahedra (Moore *et al.*, 1971). Bands H and I are similar in frequency for all Al-Gr garnets, but increase by 13 cm^{-1} with increasing Mg in Al–Py solid solutions. Band E is generally weak in intensity for most compositions and is absent in pyrope-rich garnets. Its disappearance is marked in such compositions by the emergence of band J, which is not found in the Al–Gr garnets.

Band K is intense for all compositions and careful examination of its position reveals that in Al–Gr garnets its frequency shift is linear for compositions with mol.% Gr < 20, but that there is a positive deviation from linearity at mol.% Gr > 20 (Fig. 5). The deviation is small, but greater than the experimental error (±2 cm^{-1}), and thus real. The maximum deviation is around mol.% Gr = 60–75. The deviation of this shift from linearity in Al–Gr mimics the deviation of the excess molar volumes of mixing from ideal behaviour. ΔV^{ex} is nearly zero for Al–Gr garnets at mol.% Gr < 20 and has positive values at mol.% Gr ≥ 20 (Fig. 5). Conversely, Al–Py garnets have ΔV^{mix} that are closer to being ideal and the shift of band K across the join is correspondingly linear, within the experimental uncertainties.

The asymmetric behaviour of the ΔV^{mix} curves is best explained by the equivalent site (ES) model (Newton and Wood, 1980). The model proposes that the initial substitution of a large-volume com-

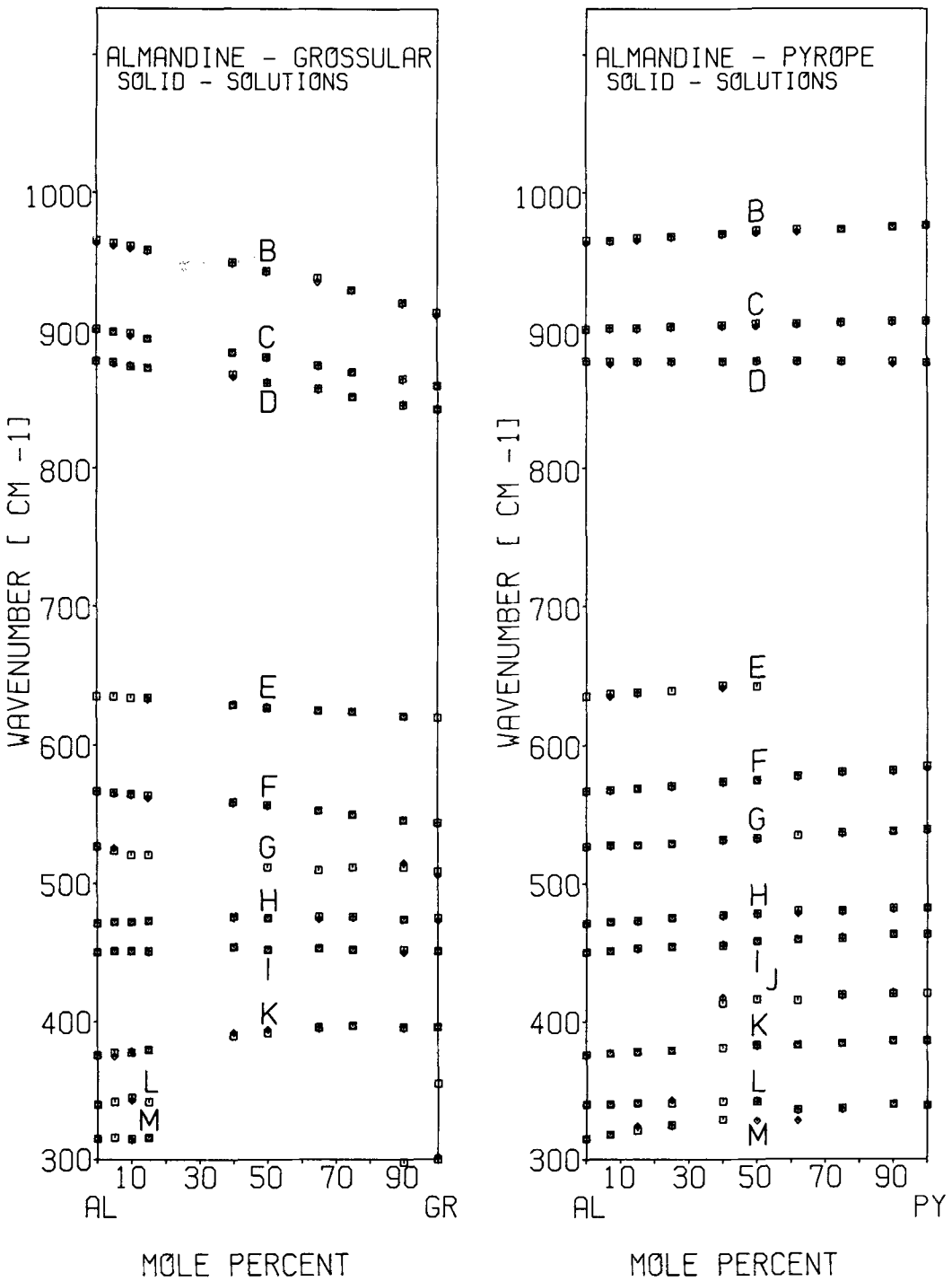

FIG. 4. Plot of position of IR bands B–M in wavenumber *vs.* composition. The size of the symbols is larger than the experimental uncertainty. Squares represent data obtained on a Perkin Elmer 580B and diamonds represent data obtained on a FTIR MX-1 Nicolet spectrometer.

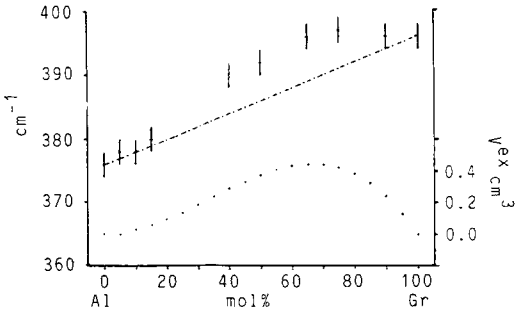

FIG. 5. A plot showing the nonlinear shift of band K in cm^{-1}, scale on the left side, compared to the excess molar volumes of mixing of almandine–grossular solid solutions in cm^3, scale on the right side. The dot-dashed line represents a linear shift between end-member almandine and grossular and the vertical lines represent the measured band positions with an experimental uncertainty of $\pm 2 cm^{-1}$. The dotted line is a two-parameter Margules best fit to the molar volumes of mixing given by all of the data in Fig. 1 for Al–Gr solid solutions, where $V^{ex} = W_{V1}X_1X_2^2 + W_{V2}X_1^2X_2$, with $W_{V1} = 3.0$ and $W_{V2} = 0.0$.

ponent (e.g. Gr) into a smaller volume host phase (e.g. Al) produces local *X*-site deformations and 'forbidden regions' surrounding them. Thus there is no excess expansion of the structure as a whole, and $\Delta V^{mix} \simeq \Delta V^{ideal}$ at low Gr contents. Continued substitution saturates the host structure, causing an interaction between the larger *X*-site cations (Ca^{2+}), until at some point excess volumes of mixing $\Delta V^{ex} > 0$, are generated.

Our IR work supports this empirical model with data which are of a microscopic nature. Vibrations in the dodecahedral *X*-site display frequency shifts which have a similar form as the molar volumes of mixing and are related to the same substitutional mechanism. The ES model has thermodynamic justifications supporting it. It can be shown that lattice vibrations govern directly the heat capacities and entropies of a given phase (Kieffer, 1979). Hence, heat capacities and third-law entropies for Al–Gr garnets probably cannot be quantitatively calculated as simple linear combinations of end-member properties.

The ES model assumes some type of ordering in the region of negative excess mixing. This could be either long or short range. Long-range order would be evidenced in a reduction of the space group symmetry of garnet. It has been proposed, based on single crystal X-ray measurements, that there is a lowering from *Ia3d* to the subgroup $I2_13$ in synthetic garnet of composition $Py_{90}Gr_{10}$ (Dempsey, 1980) and in a natural Fe-rich garnet with mol.% Gr = 8 (Cressey, 1981). Such a reduction in symmetry would increase the number of IR active bands. This is not observed in any of the grossular-poor compositions studied here. Moreover, we synthesized the composition $Al_{90}Gr_{10}$ at the relatively low-temperature of 1073 K, at 21 kbar, to induce ordering. The IR spectrum of this garnet is identical to that which was synthesized at 1423 K and shows no additional bands between 1400 and 200 cm^{-1}. This suggests that long-range structural ordering of Ca and Fe^{2+} does not occur in the samples studied here.

Burns and Huggins (1972) measured the IR spectra of a number of natural olivines in the ternary system fayalite–forsterite–tephroite. They noted shifts in frequency for bands in olivines dominated by Mg–Fe exchange (fayalilte–forsterite solid solutions). They interpreted this to indicate lack of any significant ordering of Fe and Mg between *M* (1) and *M* (2) in the olivine structure. Conversely, Mn-rich olivines displayed frequency shifts for some bands which were not linear. This was interpreted to indicate that the vibrational frequencies were site-dependent and that Mn was enriched in the *M* (2) site in olivine (Burns and Huggins, 1972). It has been shown, however, that Fe–Mg olivines do display ES behaviour in their molar volumes of mixing (Newton and Wood, 1980) and these small deviations from linear frequency shifts were probably not detected due to the lack of measurements made on samples close to the forsterite end-members. End-member forsterite was not available for study and only one other sample that was close to the Fe–Mg binary was at a composition which contained less than 20 mol.% fayalite (Burns and Huggins, 1972).

Conclusions

A recent activity-composition formulation for mineral solid solutions has also been interpreted in the context of the ES model (Powell, 1987). The most commonly used and empirically based macroscopic solution models, such as the regular or subregular models, may not be adequate to describe the thermodynamic properties such as the molar enthalpy, *H*, or molar volumes, *V*, in certain solid solutions. They cannot properly account for compositionally localized anomalies inherent in systems with ES behaviour (Powell, 1987). This problem is potentially acute in the case of garnet, because many pyrope or almandine-rich garnets contain 5–20 mol.% grossular in solid solution. This is in the region where ordering or localized volume effects may occur. Hence, these effects or volume anomalies could effect thermodynamic calculations as used, for example, in geobarometers involving garnet.

Most of the available calorimetric and experimental activity–compositional data are not precise enough to test for such small 'events'. However, IR studies are fast and precise enough to search for hidden anomalies and further measurements using high resolution FTIR spectrometers on other solid solutions are desirable.

Acknowledgements

We would like to thank Prof. Dr R. Steudel for use of the Perkin-Elmer spectrometer and Mrs R. Hilarius for technical assistance.

References

Burns, R. G. and Huggins, F. E. (1972) Cation determinative curves for Mg–Fe–Mn olivines from vibrational spectra. *Am. Mineral.* **57,** 967–85.

Cressey, G. (1981) Entropies and enthalpies of aluminosilicate garnets. *Contrib. Mineral. Petrol.* **76,** 413–9.

——Schimd, R. and Wood, B. J. (1978) Thermodynamic properties of almandine–grossular solid solutions. Ibid. **67,** 397–404.

Delany, J. M. (1981) A spectral and thermodynamic investigation of synthetic pyrope–grossular garnets. Unpub. Ph.D. thesis, Univ. Cal. Los Angeles.

Dempsey, M. J. (1980) Evidence for structural changes in garnet caused by calcium substitution. *Contrib. Mineral. Petrol.* **71,** 281–2.

Geiger, C. A. (1986) Thermodynamic mixing properties of almandine garnet solid solutions. Unpub. Ph.D. thesis, Univ. Chicago.

——Newton, R. C. and Kleppa, O. J. (1987) Enthalpy of mixing of synthetic almandine–grossular and almandine–pyrope garnets from high-temperature solution calorimetry. *Geochim. Cosmochim. Acta* **51,** 1755–63.

Haselton, H. T. and Newton, R. C. (1980) Thermodynamics of pyrope–grossular garnets and their stabilities at high temperatures and high pressures. *J. Geophys. Res.* **85,** 6973–82.

Iiyama, J. T. (1974) Substitution déformation locale de la maille et équilibre de distribution des éléments en traces entre silicates et solution hydrothermale. *Bull. Soc. Fr. Mineral. Cristallogr.* **97,** 143–51.

——and Volfinger, M. (1976) A model for trace-element distribution in silicate structures. *Mineral. Mag.* **40,** 555–64.

Kieffer, S. W. (1979) Thermodynamics and lattice vibrations of minerals: 1. Mineral heat capacities and their relationships to simple lattice vibrational models. *Rev. Geophys. Space Phys.* **17,** 1–19.

Moore, R. K., White, W. B. and Long, T. V. (1971) Vibrational spectra of the common silicates: 1. The garnets *Am. Mineral.* **56,** 54–71.

Newton, R. C. and Wood, B. J. (1980) Volume behavior of silicate solid solutions. Ibid. **65,** 733–45.

Novak, G. A. and Gibbs, G. V. (1971) The crystal chemistry of the silicate garnets. Ibid. **56,** 791–825.

O'Neill, H. St. C. and Navrotsky, A. (1984) Cation distribution and thermodynamic properties of binary spinel solid solutions. Ibid. **69,** 733–53.

Perkins, D., III (1979) Application of new thermodynamic data to mineral equilibria. Unpub. Ph.D. thesis, Univ. Michigan.

Powell, R. (1987) Darken's quadratic formalism and the thermodynamics of minerals. *Am. Mineral.* **72,** 1–11.

Tarte, P. (1965) Experimental study and interpretation of infrared spectra of silicates and germanates. *Mem. Acad. R. Belg. Sci.* 8^0 **35,** 4a–b.

[Manuscript received 20 April 1988: revised 17 October 1988]